Environmental Science: Atmospheres

ROYAL SOCIETY OF CHEMISTRY

PAPER

View Article Online
View Journal | View Issue

Cite this: *Environ. Sci.: Atmos.*, 2026, **6**, 104

Chemical composition, sources, and health risks assessment of PM_{10} and $PM_{2.5}$-bound metals at an industrial site in Nigeria

Tesleem O. Kolawole, [a] Khanneh W. Fomba, *[b] Godwin C. Ezeh, [c] Akinade S. Olatunji, [d] Khaleel A. Ghazal, [e] Falk Mothes [b] and Hartmut Herrmann *[b]

Particulate matter (PM) pollution from industrial activities is a growing environmental and public health concern, particularly in sub-Saharan Africa; where metal recycling factories (MRFs) are expanding due to increasing urbanization and metal waste generation. However, data on the chemical composition of PM and associated health risks in this region, especially in countries like Nigeria, remain limited. The present study investigates the chemical composition-including water-soluble inorganic ions, sugars, and potentially toxic elements (PTEs), and evaluates the health risks of $PM_{2.5}$ and PM_{10} collected during wet and dry seasons from an industrial hub in Nigeria dominated by MRFs. The average concentrations of $PM_{2.5}$ (27 ± 8 μg m^{-3}) and PM_{10} (109 ± 38 μg m^{-3}) in the dry season exceeded the WHO Air Quality Guidelines (15 μg m^{-3} for $PM_{2.5}$; 45 μg m^{-3} for PM_{10}), highlighting severe seasonal air quality issues. Major water-soluble ions included SO_4^{2-}, Cl^-, NO_3^-, Na^+, Ca^{2+}, and K^+, with NH_4^+, $C_2O_4^{2-}$, and Mg^{2+} present in smaller amounts. The elevated ion concentrations point to anthropogenic sources, primarily MRFs. Principal component analysis (PCA) identified crustal materials and anthropogenic emissions (from MRFs and cement factories) as major contributors to PM-bound elements. Trace metals such as Cr, Cu, Mo, Ni, Pb, and Zn showed high enrichment, with MRF activities being the dominant source. Health risk assessments using hazard quotient (HQ) and hazard index (HI) indicated non-carcinogenic risks were within acceptable limits (<1.0) for most metals in both children and adults. Carcinogenic risks were also below the permissible range (1×10^{-6} to 1×10^{-4}). However, Pb posed a near-threshold risk in children, with HQ (0.81) and HI (0.84), suggesting the need for regulatory attention to prevent potential lead toxicity in this area. Stricter regulations and monitoring of MRF activities are crucial to mitigate PM pollution and associated health risks, ensuring a safer and healthier environment for communities in Nigeria.

Received 8th April 2025
Accepted 21st October 2025

DOI: 10.1039/d5ea00045a

rsc.li/esatmospheres

Environmental significance

This study addresses the air quality and public health challenges posed by metal recycling factories (MRFs) in Nigeria focusing on the chemical composition of coarse (PM_{10}) and fine ($PM_{2.5}$) particulate matter. The study identifies MRFs as a major contributor to potentially toxic element emissions, with elevated levels of elements such as Zn, Cr, and Pb, posing localized risks. Although the non-carcinogenic and carcinogenic health risks of these elements were within permissible limits, Pb approached thresholds of concern for children living near MRFs, highlighting a potential future health risk if left unattended. The presence of levoglucosan also suggests the contribution of regional biomass burning. These findings highlight the need for activity-specific interventions and monitoring from local environmental agencies in mitigating MRF emissions and reducing exposure to harmful emissions. A recommendation could include the implementation of dust control measures, such as regular surface watering near MRFs. This research thus assists the government in improving actionable strategies to reduce local pollution practices to promote cleaner and safer air quality in the region.

[a]*Department of Geological Sciences, Osun State University, Osogbo, Nigeria. E-mail: tesleem.kolawole@uniosun.edu.ng*

[b]*Atmospheric Chemistry Department, Leibniz Institute for Tropospheric Research (TROPOS), Leipzig, Germany. E-mail: fomba@tropos.de; herrmann@tropos.de; mothes@tropos.de*

[c]*Atmospheric Research and Information Analysis Laboratory (ARIAL), Centre for Energy Research and Development (CERD), Ile-Ife 22002, Nigeria. E-mail: gcezeh@cerd.gov.ng*

[d]*Department of Geology, University of Ibadan, Ibadan, Nigeria. E-mail: akinadeshadrach@yahoo.com*

[e]*Department of Mechanical Engineering, Beijing Institute of Technology, Beijing, China. E-mail: khaleelghazal@gmail.com*

1 Introduction

The emission of inhalable particulate matter ($PM_{2.5}$ and PM_{10}) into the atmosphere is a global concern because it poses a great threat to humans and the ecosystem. The particles originate from different sources, such as combustion from vehicular emissions; city heating plants, industrial processes, construction activities, quarry activities, as well as natural processes.[1–4]

The chemical composition of PM is influenced by its sources and includes a range of inorganic compounds, such as heavy metals. It also includes organic compounds like sugars, polycyclic aromatic hydrocarbons (PAHs), and polychlorinated biphenyls (PCBs), which are potentially harmful to humans.[5] It has been established that the smaller the particle size, the farther distance it can travel in both the environment (transporting to far distances) and within human beings (penetrating the skin and respiratory tract). As a result, the lifespan of particles in the atmosphere, their deposition rates, and their chemical composition are influenced by the size of the particles. Particulate matter serves as an important indicator of air quality. It significantly affects human health and contributes to atmospheric chemistry, weather patterns, and climate dynamics.[6–8] Epidemiological studies have linked exposure to particulate matter containing heavy metals and organic compounds like PAHs and PCBs to various health issues. These health issues include respiratory disorders such as cough, asthma, bronchitis, and rhinitis, as well as other problems like renal failure and infertility.[9–11]

Nigeria, the most populous nation in Africa, continues to witness population growth and consequently an increase in urbanization. The urban centers experience accelerated air pollution because of the attendant problems associated with urbanization. This includes a notable increase in industries, vehicular traffic, and open burning of refuse. These activities are major contributors to air pollution in Nigeria and across sub-Saharan Africa.[6,12–18] In the last 2 decades, the smelting industry has been one of the fastest-growing industries in Nigeria. Exposure to their emissions has been linked to various health problems, including allergy, asthma, and cardiovascular and cardio-pulmonary diseases. Long-term exposure can also increase the risk of developing different types of cancer.[19–21] The industry mainly utilizes 100% scrap metals of different types for the production of iron/steel. In addition, nitrate and sulfate salts are mixed with quartz aggregate to reduce the veining of the metal casting prepared with a foundry mixture.[22] The industrial process is carried out in an electric-arc furnace.[20,23] This process generates emissions that are rich in non-sea salt sulfate and nitrate, black carbon, organic carbon, silica, PAH, PCB, and some potentially toxic elements (Pb, Zn, Ni, Cr, Cd, Cu, and Mn) in addition to Fe.[24–26] These potentially toxic elements are usually part of the components of the scrap metals that are volatilized during the batch process because of their low melting points.[27] Metal recycling factories (MRFs) are highly active in Nigeria, but research on their impact is limited. Specifically, there is a lack of studies conducted in the nearby communities where these factories are located. Most of the previous works in Nigeria focused on the mass concentrations of PM and their elemental compositions,[19,20,23] with no attention geared towards the attendant human health risk assessment. In other climes, researchers recently focused on the assessment of pollution caused by the smelting industry on human health in China,[1,28] and Bangladesh.[29] Their studies indicated that there is a probabilistic higher impact of potentially toxic elements (PTEs) on human health in the vicinities of MRFs than in areas with other industrial activities, such as coal fires, and areas where there are no human activities (natural existence). Also, due to poor urban planning, the factories are situated very close to residential areas. The constant exposure to the pollutants poses a major public health concern to the residents in this area. Therefore, this is among the first studies in Nigeria to research the health risk assessment of the PTEs in particulate matter on humans in the vicinity of MRFs.

The objectives of this study are to; (1) determine the mass concentration of $PM_{2.5}$ and PM_{10}in both wet and dry seasons, (2) investigate their chemical constituents such as their water-soluble ions, carbohydrates, and metals, and (3) assess the potential human health risk, including the non-carcinogenic and carcinogenic health effects of the particles.

2 Materials and methods

2.1 Site description

Particulate matter sampling was done at Likosi/Ogijo town, southwestern Nigeria. Likosi/Ogijo is a community with approximately 150, 000 inhabitants and 50 km^2 in size. The study area is about 5 km west of Ikorodu and 50 km north of the coastal city of Lagos, which is the commercial hub of Nigeria and one of the most populated cities in the country. The choice fell on this area because the community accommodates the largest colony of metal recycling factories (MRFs) in Nigeria, numbering about 15 big plants within a 1 km stretch. The metal recycling factories (MRFs) are located in this community because of the area's major gas pipelines. These pipelines provide a convenient source of fuel for the industries to generate electricity for their smelting processes. In addition, other manufacturing industries such as cement and petrochemical companies are situated in this area, hence, the choice of this location (Fig. 1). The sampling station was located between 2 big plants; about 150 m south of one plant and 100 m north of the second plant (6°44′42.8″N, 3°31′36.4″E).

The geology of the study area is mainly dominated by Tertiary to Recent Coastal Plain Sands, which typifies the sedimentary basin of southwestern Nigeria. It is composed of a repetitive succession of clay and sandy horizons. The clay horizon appears mostly reddish-brown and, in some places, dirty-white, while the sandy horizon ranges from very fine to coarse and gravelly in texture. Minor peat and ferruginous sandstone layer occurrences have also been reported in the area.[20]

The study area experiences warm temperatures throughout the year, ranging from 23.0 °C to 33.0 °C. The annual rainfall varies greatly, with lows of around 10 mm in the dry season (January) and highs of up to 350 mm in the wet season (July). The precipitation frequency is about 100 events annually, mainly between April and October.[30] The wind direction is typically southerly, and the wind speed ranges from 2 to 7 km h^{-1}. The metrological information was collected from the nearby weather station in Sagamu (Table 1).

2.2 Sample collection

The sample was collected with a Gent stack filter unit (SFU) sampler, manufactured by the Institute of Nuclear Sciences,

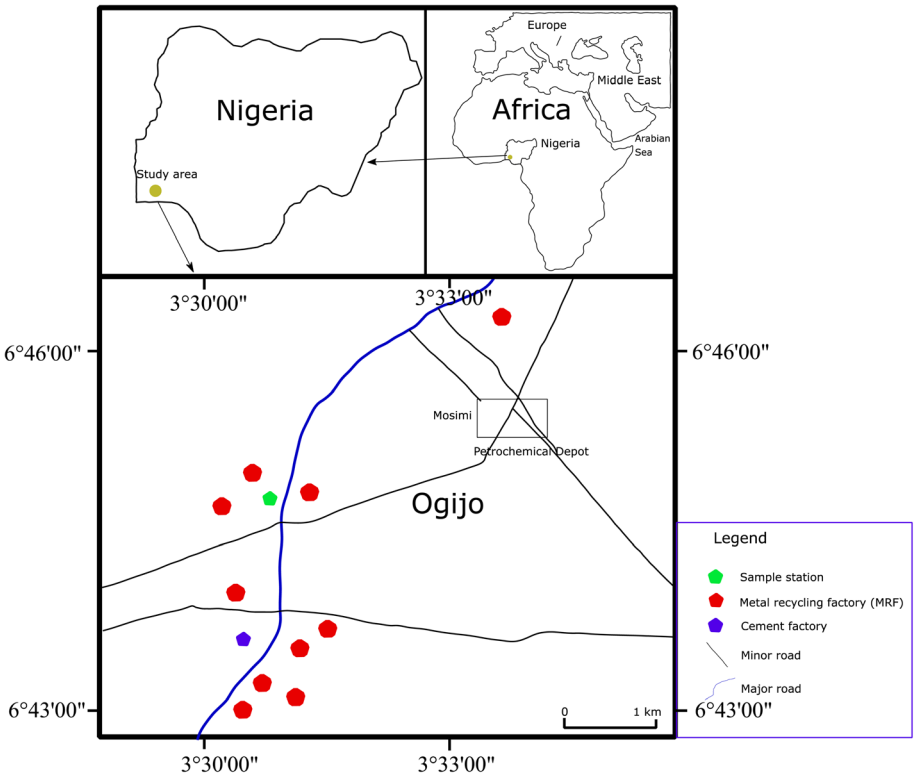

Fig. 1 Location of the study area.

Table 1 Metrological data

Sample stations	Collection date	Collection time	Weekly average temperature (°C)	Weekly average humidity (%)	Weekly average wind speed (km h^{-1})	Weekly wind direction
Wet season	October3–10, 2020	6:00 am–6:00 am	30	90	3	Southeast
Dry season	October21–27, 2021	6.00:am –6:00 am	32	78	5	Southeast

Gent University, Belgium. The sampler is a low-volume sampler with a flow rate of 16–18 $Lmin^{-1}$. The sampler can collect fine ($PM_{2.5}$) and coarse (PM_{10}) fractions of particulate matter. In-depth descriptions of the sampler have been documented elsewhere.[31,32] The samples were collected using pre-weighed Whatman Nuclepore filters that had been conditioned at a steady temperature and humidity. The filters were conditioned for 24 hours at approximately 25 °C and 50% humidity, following the method used by Obioh *et al.* and Ezeh *et al.*[31] The exposed filters underwent triplicate measurements with a digital micro-weighing balance (Sartorius, Gottingen, Germany) with 0.001 mg reading resolution. The balance was calibrated using the automated isoCAL function to maintain accuracy. The selection of nucleopore filter is based on their low intrinsic trace element blank, making them suitable for trace metal analysis, as reported in the literature.[33] It is also on the basis of their non-hygroscopic properties and chemical stability, which can improve the analytical quality of the analyses.[8] The first filter in the stack has 0.8 mm pores for the PM_{10} fractions, while the second filter has 0.4 mm for the $PM_{2.5}$ fractions. Sample collection was performed at the ground level with an inlet height of 1.7 m, equivalent to an individual's average nose height. The sampling time was 24 hours (starting from 6:00 to 6:00 the next day) for a week in the wet season (October 2020) and a week in the dry season (March 2021).

2.3 Laboratory analysis

The samples collected were examined for their content of water-soluble ions, carbohydrates, and metals. For ion analysis, 25% of the PM_{10} and $PM_{2.5}$ filters were extracted with 30 ml of Milli-Q water (>18 M Ω cm). The extraction process involved a sequence of 15 minutes of shaking, 15 minutes in an ultrasonic bath, and another 15 minutes of shaking. Before measuring the ions, the sample extracts were passed through a 0.45 μm one-way syringe filter to eliminate any insoluble impurities. The ion measurement was conducted using a standard ion chromatography method (ICS3000, DIONEX, USA) equipped with automatic eluent generation, utilizing KOH for anions and methanesulfonic acid (MSA) for cations such as Na^+, NH_4^+, K^+, Mg^{2+}, Ca^{2+}, as well as anions including Cl^-, NO_3^-, SO_4^{2-}, and $C_2O_4^{2-}$.

This methodology has been detailed in the work of Fomba *et al.*[33] The sugar analysis was also done on filter extracts using the IC, and details have been reported elsewhere.[34] For the metal analysis, about 0.25 cm^2 Nucleporefoil was cut and placed on a 3 cm Total reflection X-ray fluorescence spectroscopy (TXRF) sampler carrier disc. The sample was spiked with a Gallium internal standard and allowed to dry on a hot plate, and the sample carrier with the sample was thereafter analyzed using TXRF (Picofox S2, Bruker, Germany). This study detected and discussed 12 elements, including Ca, Cr, Cu, Fe, K, Mn, Mo, Ni, Pb, Sr, Ti, and Zn. The details of the metal analytical methods have been reported by Fomba *et al.*[35] Although theoretically, TXRF can analyze elements from Al to Bi but for this study, the undiscussed elements were not detected. The elemental detection limit has been described in former studies.[33,35] The Quality assurance and quality control procedures were conducted using standard protocols reported in numerous literature.[35,36]All measurements were accompanied by blank measurements of both batch samples and field blanks, which were subtracted from the analytical values to obtain the values above background concentrations. Also, the instruments were calibrated to ensure a good identification of the specific compound, such as Na^+, SO_4^{2-}, NH_4^+, Ca^{2+}, and other water-soluble ions, during the ion chromatography analysis, with a similar procedure applied to trace metals, sugar, and organic carbon analysis.

2.4 Health risk assessment

The study estimated the health risk of air pollution for some selected metals (Cr, Cu, Fe, Mn, Ni, Pb, and Zn) for both children and adults by employing the USDOE[37] and USEPA[38] models. These elements were selected for the assessment because of their known and established health effects. The models proposed the risk for both non-carcinogenic and carcinogenic impacts of PTEs, as reported in the following subsection.

2.5 Non-carcinogenic risk

A quantitative assessment of the non-carcinogenic risks associated with PTEs in particulate matter (PM_{10} and $PM_{2.5}$) was conducted, focusing on three primary exposure pathways: ingestion, inhalation, and dermal contact. This evaluation utilized hazard quotients (HQs) for each metal analyzed. The calculations were derived from the specified equations below:

For chronic daily intake (CDI) for the three pathways:

$$CDI_{Ing} = \frac{C \times IngR \times EF \times ED}{BW \times A_{Tnc}} \times 10^{-6} \quad (1)$$

$$CDI_{Inh} = \frac{C \times InhR \times EF \times ED}{PEF \times BW \times AT} \quad (2)$$

$$CDI_{der} = \frac{C \times SA \times AF \times ABSd \times EF \times ED}{BW \times AT} \times 10^{-6} \quad (3)$$

$$HQ = \frac{CDI}{RfD} \quad (4)$$

The definitions of each term can be found in Table 2. Additionally, Table S1 provides the reference dose (RfD) values (mg kg^{-1} day^{-1}) for the specified potentially toxic elements (PTEs).[39,40] The hazard index (HI) is calculated as the cumulative sum of the hazard quotients (HQ) and is utilized to evaluate the overall non-carcinogenic risk associated with the measured PTEs. The formula for HI is as follows:

$$HI = \Sigma HQ = \Sigma CDI/RfD \quad (5)$$

Values for both the Hazard Quotient (HQ) and Hazard Index (HI) that are less than 1 indicate a level of non-carcinogenic risk that is considered acceptable. In contrast, if either the HQ or HI exceeds 1, it indicates a potential health risk due to surpassing the acceptable limits for non-carcinogenic exposure. The terms used in eqn (4) and (5) are detailed in Table 2.

2.6 Carcinogenic risk assessment

The carcinogenic risk (CR) was assessed based on the probability of developing cancer throughout a person's lifetime. The CR was determined for three distinct pathways as outlined below:[3,38,39]

$$CR_{Ing} = \frac{C \times IFS \times RBA \times CSFo}{A_{Tnc}} \times 10^{-6} \quad (6)$$

$$IFS = \left(EF \times EDa \times \frac{IRSa}{BWa}\right) + \left(EF \times EDc \times \frac{IRSc}{BWc}\right) \quad (7)$$

$$CR_{der} = \frac{C \times DFS \times ABSd \times CSFo}{AT \times GIABS} \times 10^{-6} \quad (8)$$

$$DFs = \left(EF \times EDa \times SAa \times \frac{AFa}{BWa}\right) + \left(EF \times EDc \times SAc \times \frac{AFc}{BWc}\right) \quad (9)$$

$$CR_{Inh} = \frac{C \times EF \times ED \times IUR \times 1000}{AT \times PF} \quad (10)$$

The total carcinogenic risk (TCR) can be expressed using the following equation:

$$TCR = CR_{ing} + CR_{der} + CR_{inh} \quad (11)$$

Details regarding the parameters and the specific factor values used for risk assessment are provided in Tables 2 and S1.

2.7 Statistical analysis

Statistical analysis of chemical composition data involved calculating descriptive statistics and performing one-way analysis of variance (ANOVA) using SPSS to identify differences in composition levels across the PM samples. Correlation analysis and principal component analysis (PCA) with Varimax rotation and Kaiser Normalization were also applied to assess relationships between chemical sources and variables in the PM.

Table 2 Definitions of parameters and values of the variables for estimating human exposure to soil and sediment

Symbols	Units	Definition value	Value	Ref.
CDI	mg kg^{-1} day^{-1}	Chronic daily dose through ingestion, inhalation, and dermal contact with substrate particles	—	USDOE[37]
C	mg kg^{-1}	Concentration of heavy metals in substrate	—	
IngR	mg day^{-1}	Soil and sediment ingestion rate for the receptor resident	200 (child) 100 (adult)	USDOE[37]
InhR	m^3 day^{-1}	Soil inhalation rate for receptor resident	7.63 (child) 20 (adult)	USDOE[37]
EF	day $year^{-1}$	Exposure frequency	350 (resident) 75 (recreations)*	USDOE[37]
ED	year	Exposure duration	30 (resident, recreation) 6 child (resident)	USDOE[37]
BW	kg	Average body weight	42.4 (child) 70.8 (adult)	USDOE[37]
AT_{nc}	D	Average time for non-carcinogenic effects	ED × 365 (resident and recreation)	USDOE[37]
PEF	m^3 kg^{-1}	Soil to air particulate emission factor	1.36×10^9	USDOE[37]
SA	cm^2 $event^{-1}$	Skin surface area available for exposure	2800 (child) 5700 (adult)	USDOE[37]
AF	mg cm^{-2}	Soil to skin adherence factor	0.2 (child) 0.07 (adult)	USDOE[37]
ABSd	Unitless	Dermal absorption factor	0.03 (As); 0.001 (other heavy metals)	USDOE[37]
RfD_{ing}	mg kg^{-1} day^{-1}	Chronic oral reference dose	Table S1	Table S1
RfC_{inh}	mg m^{-3}	Chronic inhalation reference concentration	Table S1	Table S1
RfD_{der}	mg kg^{-1} day^{-1}	Chronic dermal reference dose, = RfDingxABSgi	Table S1	Table S1
GIABS		Gastrointestinal absorption factor	Table S1	Table S1
CSFo		Oral slope factor	Table S1	Table S1
IUR		Inhalation unit risk	Table S1	Table S1

3 Results and discussion

3.1 $PM_{2.5}$ and PM_{10} concentration

Fig. 2 provides an overview of the daily mass concentrations of $PM_{2.5}$ and PM_{10}, as well as the percentage ratios of $PM_{2.5}$ to PM_{10} during the wet and dry seasons. In the wet season, $PM_{2.5}$ concentrations ranged from 5 to 16 μg m^{-3}, while PM_{10} levels fluctuated between 16 and 76 μg m^{-3}. In contrast, the dry season saw $PM_{2.5}$ concentrations between 12 and 36 μg m^{-3}, with PM_{10} concentrations ranging from 42 to 158 μg m^{-3}. The average mass concentrations for $PM_{2.5}$ were 11 ± 4 μg m^{-3} during the wet season and 27 ± 8 μg m^{-3} in the dry season. For PM_{10}, the averages were recorded at 46 ± 26 μg m^{-3} in the wet season and 109 ± 38 μg m^{-3} in the dry season. The aerosol mass

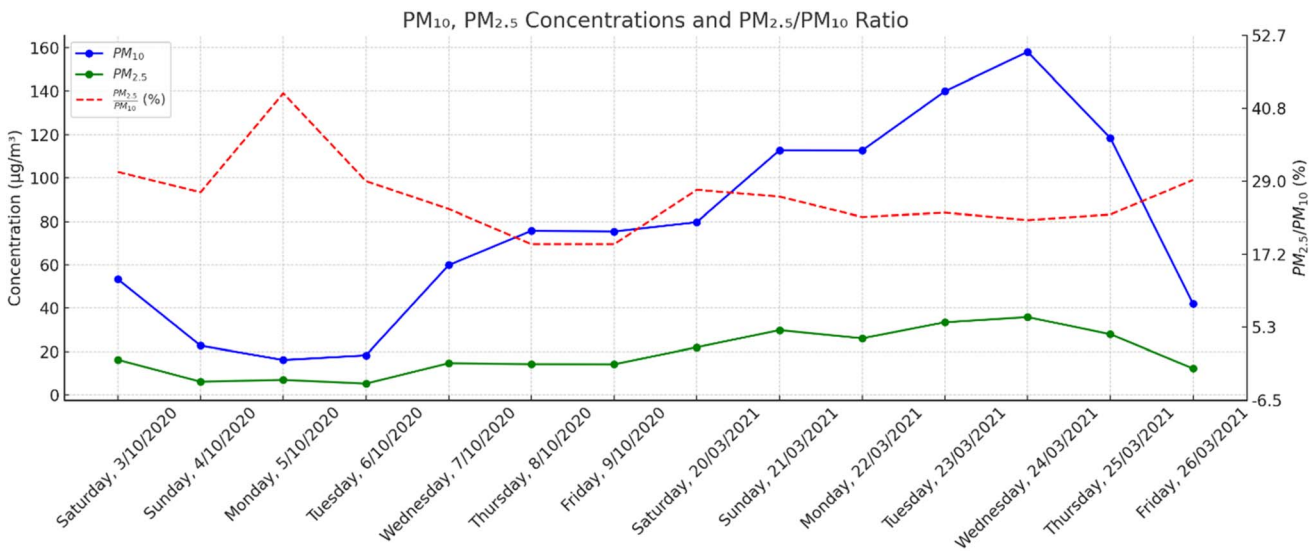

Fig. 2 Daily mass concentration of PM and the ratios of the size fractions ($PM_{2.5}/PM_{10}$).

showed considerable variability, with $PM_{2.5}$ reaching a minimum of 5 μg m^{-3} in the wet season and PM_{10} peaking at 158 μg m^{-3} in the dry season. Fig. 2 depicts the time series data for the mass concentrations of $PM_{2.5}$ and PM_{10} throughout both seasons. The highest daily concentration of $PM_{2.5}$ was observed on March 24, 2021, which was a dry day (no precipitation) with moderate wind speed, and the lowest daily concentration was observed on October 6, 2020, was also a day with low wind speed but high precipitation.

Likewise, the highest and the lowest daily concentrations of PM_{10} in the dry season were observed on March 24, 2021 (dry season) and October 5, 2020 (wet season), respectively. The average daily $PM_{2.5}$ levels did not surpass the 24 hours air quality guideline (AQG) limit set by the World Health Organization (WHO) during the wet season. In contrast, during the dry season, $PM_{2.5}$ levels exceeded the WHO AQG on more than 33% of the sampling days.PM_{10} exceeded the WHO AQG on most days in the wet and dry seasons. The average $PM_{2.5}/PM_{10}$ ratios in the wet and dry seasons were 27% and 25% respectively. The minimum value was observed on October 8, 2020 and October 9, 2020 (19%) in the wet season, while the maximum $PM_{2.5}/PM_{10}$ ratio of 44% was also obtained in the wet season (October 5, 2020). This result suggests a dominance of coarse-mode particles over fine-mode particles. The high ratio observed on October 5, 2020, and the generally higher values during the wet season are attributed to low wind speeds. These conditions, combined with wet surfaces, reduce the resuspension of coarse-mode dust particles from roads. Thus, one can conclude that precipitation washes off the coarse mode particles strongly than the fine mode particles and suppresses the coarse mode fraction of the particles, *via* washout and prevention of road dust resuspension.

The PM concentrations observed in this study were analyzed in relation to findings from previous research conducted in Nigeria and other global locations (Table 3). It was noted that the average $PM_{2.5}$ levels during the wet (11 μg m^{-3}) and dry (27 μg m^{-3}) seasons were lower than those documented in Ile-Ife, Nigeria,[19] and other regions. Additionally, the average PM_{10} concentration during the wet season (46 μg m^{-3}) was found to be lower than the values reported by Owoade *et al.*,[19] yet comparable to those recorded in Dushanbe, Tajikistan (Table 3).[4,41]

In the dry season, PM_{10} levels were also lower than those reported in Ile-Ife and Ikorodu,[19,23] Nigeria, as well as in Chengdu, China.[1] Conversely, the PM_{10} concentrations in this study exceeded those found in Taiwan,[42,43] Zhuzhou, China,[44] and Seoul, South Korea.[45] The high concentrations were mainly due to the fugitive dust resuspension from the soil by vehicular movement, coupled with the industrial emission of aerosol particles from the MRFs in the study area. This assertion was also corroborated by Owoade *et al.*,[19] and Olatunji *et al.*,[20] who found similar high concentrations when they sampled at other industrial sites in Nigeria.

3.2 Ionic components

3.2.1 Coarse fractions. The results of water-soluble ions of $PM_{10}$are presented in Table 4. It was observed that the most notable ions in order of their abundance were chloride (Cl^-) > nitrate (NO_3^-) > sulfate (SO_4^{2-}) >sodium (Na^+) > calcium (Ca^+) > potassium (K^+) > ammonium (NH_4^+) > oxalate ($C_2O_4^{2-}$) > magnesium (Mg^{2+}) based on their average concentrations. There is significant variation between the major ions and minor ions in both the dry and wet seasons. The values range from 66 ng m^{-3} (the lowest, observed for K^+) to 374 ng m^{-3} (the highest, observed for SO_4^{2-}) among the major ions (Cl^-, SO_4^{2-}, NO_3^-, Na^+, Ca^{2+}, and K^+), in PM_{10} in the dry season. The minor ions, NH_4^+, $C_2O_4^{2-}$, and Mg^{2+}, had average concentrations ranging from 18 ng m^{-3} (NH_4^+) to 29 ng m^{-3} ($C_2O_4^{2-}$) in the wet season, and from 51 ng m^{-3} (Mg^{2+}) to 91 ng m^{-3} (NH_4^+) in the dry season. The major ions, especially the SO_4^{2-}, NO_3^-, Na^+, $Ca^{2+}$and K^+ were sourced from primary emission from industrial combustion by the MRF plants. It was established that sulfate and or nitrate salts, such as sodium sulfate, sodium nitrate, calcium sulfate, calcium nitrate, potassium sulfate, and potassium nitrate, are employed as the sand additive of the foundry mix during iron and steel production.[22] The sources of the Cl^- and the minor ions such as NH_4^+, $C_2O_4^{2-}$, and Mg^{2+} were attributed to industrial combustion and sea salt aerosol.[47,48]

3.2.2 Fine fractions. Similarly, the results of the concentrations of the water-soluble ions in $PM_{2.5}$ in both the wet and dry seasons are presented in Table 4. In terms of their average concentrations, the ions decrease in the following order: Cl^- >

Table 3 Comparison of average concentrations $PM_{2.5}$ and PM_{10} in μg/$m^3$of this study with previous works

Places	$PM_{2.5}$	PM_{10}	Ref.
Ogijo, Nigeria (wet season)	11	46	This study
Ogijo, Nigeria (dry season)	27	109	This study
Chengdu, China	—	174	Cheng, *et al.*[1]
Dushanbe, Tajikistan	—	45	Fomba *et al.*,[4,41]
Ife, Nigeria	223	381	Owoade *et al.*[19]
Lagos, Nigeria	142	2805	Owoade *et al.*, 2009(ref. 23)
Taiwan	51	91	Chu *et al.*[42]
Changhua county, Taiwan	34	52	Hsu, *et al.*[43]
Zhuzhou, Hunan province, China	114	62	Zhang *et al.*[44]
Seoul, South Korea	—	88	Lim *et al.*[45]
Milan, Italy	38	113	Zoran *et al.*[46]

Table 4 The statistical summary of soluble-ions, carbohydrates, and metals of $PM_{2.5}$ and PM_{10} in both the wet and dry seasons in the study area. All concentrations are measured in ng m^{-3}[a]

		Coarse (PM_{10})				Fine ($PM_{2.5}$)				
		Wet season		Dry season		Wet season		Dry season		
		Mean ± Std	Range	Mean ± std	Range	Mean ± Std	Range	Mean ± std	Range	*P* value
Ions	Chloride	254 ± 96	139–405	1176 ± 392	599–1891	14 ± 6	3–20	104 ± 115	26–351	***
	Nitrate	241 ± 73	142–337	690 ± 367	292–1188	35 ± 24	17–81	41 ± 26	12–92	***
	Sulfate	374 ± 79	268–456	600 ± 319	234–1216	55 ± 21	29–90	71 ± 35	37–135	**
	Oxalate	29 ± 12	11–49	81 ± 44	28–157	3 ± 1	0–4	8 ± 3	4–15	**
	Sodium	135 ± 45	98–228	330 ± 131	197–580	18.6 ± 5.4	9–27	34 ± 25	17–87	**
	Ammonium	18 ± 11	4–30	95 ± 75	11–224	19.4 ± 5.3	11–24	14 ± 4	8–20	**
	Potassium	66 ± 19	37–93	127 ± 61	45–204	18 ± 10	5–35	32 ± 28	7–87	**
	Magnesium	21 ± 6	15–34	51 ± 26	24–99	1.7 ± 1.6	0.4–4.1	1.7 ± 2.2	0.5–6.5	**
	Calcium	112 ± 15	95–133	189 ± 101	63–345	10 ± 13	1–35	7 ± 5	2–17	**
Sugar	Levoglucosan	19 ± 12	6–39	126 ± 99	28–306	3 ± 2	0–5	5 ± 4	0–13	***
	Mannosan	191 ± 47	103–241	212 ± 29	179–265	453 ± 61	349–520	389 ± 34	348–447	***
Metals	K	101 ± 17	80–131	190 ± 66	115–311	61 ± 11	48–80	74 ± 16	53–102	**
	Ca	150 ± 40	113–234	272 ± 113	155–468	92 ± 48	59–201	109 ± 28	74–140	**
	Ti	5.2 ± 2.6	1.9–8.7	34.7 ± 18.6	4.8–57.7	1.1 ± 1.6	BDL-4.0	4.2 ± 3.1	BDL-9.4	**
	Cr	2.8 ± 1.0	1.9–4.6	6.2 ± 2.7	3.2–11.5	2.3 ± 0.5	1.5–3.1	2.6 ± 0.8	1.9–4.0	***
	Mn	3.3 ± 1.2	1.8–5.7	30.9 ± 16.2	11.9–60.0	BDL	BDL	1.7 ± 1.4	BDL-3.8	**
	Fe	77 ± 26	53–126	733 ± 406	221–1377	20 ± 8	10–34	54 ± 23	19–76	**
	Ni	2.1 ± 0.7	1.3–3.3	4.1 ± 2.1	2.9–8.8	1.7 ± 0.5	1.1–2.4	1.8 ± 0.3	1.6–2.3	**
	Cu	4.6 ± 1.6	2.7–7.3	13.8 ± 7.7	6.8–27.9	1.6 ± 0.4	1.1–2.1	2.0 ± 0.7	1.4–3.3	**
	Zn	243 ± 123	70–383	2411 ± 1216	1422–4810	23 ± 17	6–55	174 ± 161	48–509	***
	Sr	1.8 ± 1.5	BDL-3.6	3.9 ± 2.0	2.2–8.0	2.2 ± 0.8	0.6–3.0	2.5 ± 0.9	BDL-3.3	*
	Mo	53 ± 32	0–91	116 ± 107	35–291	2.8 ± 7.3	BDL-19.3	13.2 ± 12.7	BDL-27.2	***
	Pb	643 ± 335	342–1356	1649 ± 1288	469–3806	35 ± 17	12–55	89 ± 52	14–162	***

[a] BDL = Below Detection Limit, Levels of significance: ***$p < 0.001$, **$p < 0.01$, *$p < 0.05$, ns—not significant.

$SO_4^{2-} > NO_3^- > Na^+ > K^+ > NH_4^+ > C_2O_4^{2-} > Ca^+ > Mg^{2+}$. The lowest average value of the ions was 3.0 ng m^{-3}, which was observed for $C_2O_4^{2-}$while the highest value of 55 ng m^{-3} was found for SO_4^{2-}in $PM_{2.5}$ in the wet season. However, in the dry season, the lowest average concentration was observed for Mg^{2+} (1.7 ng m^{-3}), and the highest value was found for Cl^- (104 ng m^{-3}) in $PM_{2.5}$. The sources of these ions, such as Cl^- were attributed to industrial combustion and sea salt aerosol, while the oxidation of SO_2 and NO_X emitted from MFR will form SO_4^{2-} and NO_3^-in the atmosphere, respectively.[48,49]

3.3 The interrelationship between ionic species

3.3.1 Coarse fraction. A strong positive correlation among the three major anionic species (Cl^-, NO_3^-, and SO_4^{2-}) was observed in this study, especially in PM_{10} and across the seasons. For example, a strong positive correlation exists between SO_4^{2-} and Cl^- ($r^2 = 0.81$), SO_4^{2-} and NO_3^- ($r^2 = 0.86$), and Cl^- and NO_3^- ($r^2 = 0.87$) (Table S2). The correlation coefficient (r) was positively strong between Cl^- and NO_3^-(0.67), $Cl^-$and SO_4^{2-}(0.72), and $SO_4^{2-}$and NO_3^-. This implied that they may have had a common origin, which could be attributed to anthropogenic emissions of their salts from the MRFs in the study area.

Similarly, strong positive correlation also exists among Na^+–Ca^{2+}–Mg^{2+} ($r^2 = 0.72$–0.92),K^+ – Mg^{2+}–Ca^{2+} ($r^2 = 0.80$–0.92), Mg^{2+}–Ca^{2+} ($r^2 = 0.92$) (Table S2) in PM_{10} in both wet and dry seasons. This also implied that the elements had a common origin or were similarly affected by precipitation and weather conditions. Furthermore, the strong positive correlations between the anionic and cationic species presented in Table S2 indicate the similarity in the sources of SO_4^{2-} and K^+–Na^+–Mg^{2+}–Ca^{2+}, in PM_{10} across the seasons, as also observed elsewhere.[48,49] It was established that sulfate or nitrate salts, such as sodium sulfate, sodium nitrate, calcium sulfate, calcium nitrate, potassium sulfate, and potassium nitrate, are employed as the sand additive of the foundry mix during iron and steel production.[22] Thus, the observed correlation between these ions is likely linked to emissions emanating from these activities.

3.3.2 Fine fraction. Also, a strong positive correlation exists among anionic species (Cl^-, NO_3^-, and SO_4^{2-}) in $PM_{2.5}$ (Table S2). Similarly, the correlation coefficient between the cations and anions in $PM_{2.5}$ was strong for only Mg^{2+} and NO_3^- ($r^2 = 0.83$), Na^+ and Cl^- ($r^2 = 0.93$), and $Ca^{2+}$and NO_3^- ($r^2 = 0.68$), and generally weak for other ions (Table S2). This suggests the $MgCl_2$ and NaCl particles are in the fine mode.

The strong relationship/association suggested that salt mixtures of nitrate and sulfate were significantly emitted into the atmosphere in the study area through industrial processes from the MRF plants.

3.4 Sugar

3.4.1 Coarse fraction. The major carbohydrate substances observed in the PM were Levoglucosan and Mannosan. Their peak concentrations were 305 ng m^{-3} (Levoglucosan) and 447

ng m^{-3} (Mannosan) during the dry season on March 22, 2021. In contrast, the minimum values of 6.3 ng m^{-3} (Levoglucosan) and 179 ng m^{-3} (Mannosan) were recorded during the wet season on October 4, 2020 (Table 4). Similarly, the disparity in the average concentrations in the wet season (19 ng m^{-3}) and the dry season (126 ng m^{-3}) shows a significant variation in the budget of this substance in both seasons. Both Levoglucosan and Mannosan have been established to be major biomarkers for tracking biomass burning in the atmosphere.[36,50–54] Therefore, the very high concentrations of Levoglucosan and Mannosan, especially in the dry season, were attributed to the anthropogenic activity of wood burning through outdoor cooking by the locals, a practice that is common in the study area. Viana *et al.*,[52] reported an average Levoglucosan concentration of 129 ng m^{-3} in PM_{10} during episodic bush burning in Valencia (Eastern Spain). This value was similar to the average value observed in this study during the dry season, which was attributed to biomass burning. Stevens *et al.*[53] compared Levoglucosan and Mannosan ratios in sediments and corresponding aerosols from recent Australian fires, highlighting the use of these compounds as tracers for biomass burning emissions. High concentrations of K^+, a tracer for biomass/wood burning, were observed in this study. K^+ showed strong correlations with levoglucosan, with r^2 values of 0.98 in the dry season and 0.68 in the wet season. This suggests that they have a common origin, which is ascribed to their emission from biomass burning. In addition, the positively strong correlation between Levoglucosan and Oxalate ($r^2 = 0.93$) is also an indication of its origin from the same source (wood burning) as suggested by Viana *et al.*,.[52] Levoglucosan showed strong positive correlations with NO_3^- ($r^2 = 0.87$), Ca^{2+} ($r^2 = 0.72$), and SO_4^{2-} ($r^2 = 0.84$). These correlations suggest that biomass burning likely contributed to the levels of these species, in addition to emissions from metal recycling facilities (MRFs).

3.4.2 Fine fraction. The concentrations of Levoglucosan were below 5.5 ng m^{-3} in the wet season and 13 ng m^{-3} in the dry season (Table 4). The highest value was reported in the dry season. The highest value of Mannosan 520 ng $m^{-3}$was reported during the wet season. Simoneit *et al.*[45] and Schkolnik *et al.*[46] reported higher Levoglucosan values than those found in this study. Their observed high concentrations were attributed to wood burning, similar to the source identified in this study. The lower Levoglucosan concentrations in the wet season and fine mode likely result from reduced biomass burning activities and fewer coarse particles in the atmosphere for the compound to adhere to. This reduction in coarse particles limits Levoglucosan's contribution to the coarse mode fraction. Levoglucosan in this study was predominantly found in the coarse mode and at higher concentrations during the dry season. The higher coarse mode fraction during the dry season provided surfaces for Levoglucosan to condense onto. This, combined with reduced atmospheric washout, contributed to the increased levoglucosan levels in the dry season.

3.5 Metals

3.5.1 Metals distribution. Twelve (12) metals were measured in both $PM_{2.5}$ and PM_{10} across the wet and dry seasons, in October 2020 and March 2021, respectively. The statistical summary (average, standard deviation, minimum, and maximum values) of the metals, which include Ca, Cr, Cu, Fe, K, Mn, Mo, Ni, Pb Rb, Sr, Ti, and Zn, is presented in Table 4.

3.5.1.1 Coarse mode (PM_{10}). All the major elements, such as Ca, Fe, and K, that are often reported to have crustal signatures, showed high concentrations across the wet and dry seasons for the coarse particles.

The highest concentrations of Ca (234 and 468 ng m^{-3}), Fe (126 and 1377 ng m^{-3}), and K (131 and 311 ng m^{-3}) in both wet and dry seasons were observed on October 4, 2020 (wet season) and March 22, 2021 (dry season) (Table 4). These days correspond to the periods with the highest PM concentrations. The difference between the minimum and maximum values showed that there is significant variation of these metals across the seasons. There is a significant difference between the average concentrations of Ca (272 ± 113 ng m^{-3}), Fe (733 ± 406 ng m^{-3}), and K (190 ± 66 ng m^{-3}) in the dry season than their respective values in the wet season (Ca-150 $\pm$ 40, Fe-77 $\pm$ 26, and K-101 $\pm$ 17 ng m^{-3}) in PM_{10}.

Also, from the one-way ANOVA results, statistically significant differences ($p < 0.001$, $p < 0.01$) were revealed in the concentrations of all the metals, particularly between $PM_{2.5}$ and PM_{10} during the dry season, except for Sr ($P < 0.05$) (Table 4), were observed. Additionally, significant differences were observed between coarse and fine particles in both wet and dry seasons, as well as between fine particles in the wet and dry seasons. These findings suggest that metal concentrations vary substantially depending on particle size and season. These metals have been reported in Nigeria,[19,20] with a similar soil type to be a major component of the soil in the study area; hence, their preponderance in the coarse mode fraction is explicable. Therefore, their presence in the atmosphere is mostly a result of the fugitive soil dust that is resuspended by wind and vehicular movement into the atmosphere.

However, their occurrence in the study area could also be a result of emissions from the MRF, which may be responsible for Fe and K. The values of these metals for the PM_{10} observed in this study were comparable with other studies in Nigeria,[31,55] Tanzania,[54,56] and Brazil[57] with similar soil types, where they also reported high values of Ca. This assertion was supported by previous work in a similar environment in Nigeria.[19] The findings suggest that K and Fe were among the major elements associated with emission during metallurgical production. These metallurgical factories emit Fe and other substances from their furnaces, this assertion was supported by previous work in a similar environment in Nigeria.[19,20,23] The respective average concentrations of Mn, Rb, Sr, and Ti in both wet and dry seasons are 3.3 and 31, 0.5 and 0.8, 1.8 and 3.9, 5.2 and 35, all expressed in ng m^{-3}. Therefore, they decrease in the following descending order: Mn > Ti > Sr > Rb. The highest concentrations of Mn, Ti, Sr, and Rb in both the wet (5.7 ng m^{-3}, 8.7 ng m^{-3}, 3.6 ng m^{-3}, and 0.9 ng m^{-3}) are lower than their corresponding values in the dry (60 ng m^{-3}, 58 ng m^{-3}, 8.0 ng m^{-3}, and 1.8 ng m^{-3}) seasons. These metals were also attributed to their crustal contributions from the local soil resuspension.

The most notable trace metals in this study were Pb and Zn; these metals have high concentrations in these size fractions, and they are predominantly from anthropogenic emissions from combustion processes.[58] Their respective mean concentrations for both the wet season (643 and 243 ng m^{-3}) and dry season (1649 and 2411 ng m^{-3}) were higher in comparison to the reported concentrations of other studies in China,[44] Mexico,[59] Tajikistan,[4,41] and Brazil.[57] However, the high values of these metals agreed with previous work in a similar environment in Nigeria,[19,23] where the mean Pb concentrations were also high (between 2.4–5.3 μg m^{-3}). The elevated concentrations were linked to the metallurgical production of iron and steel, as industrial emissions from metal recycling facilities in the study area play a significant role. This phenomenon is associated with the alloying materials and residual paints from the scrap metals, which tend to become volatile during the smelting process.

In addition to the anthropogenic Pb and Zn, the presence of Cr, Cu, Mo, and Ni in both seasons in this fraction were associated with the activities of the MRFs. These metals (Cr, Cu, Mo, and Ni) have also been reported to be tracers for the ferrous metal industryemissions.[19,59] They were observed in wet (2.8, 4.6, 53.0, and 2.1 ng m^{-3}, respectively) and dry (6.2, 13.8, 116, and 4.1 ng m^{-3}, respectively) seasons.

3.5.1.2 Fine mode ($PM_{2.5}$). Similarly, the average concentrations of Fe (20 ng m^{-3}), Ca (92 ng m^{-3}), and K (61 ng m^{-3}) in the wet season were lower than their corresponding values of 54 ng m^{-3}, 109 ng m^{-3}, and 74 ng m^{-3}, respectively, in the dry season (Table 4). Other metals, according to their abundance, were Zn > Pb > Mo > Ti > Cr > Sr > Cu > Ni > Mn > Rb, and varied across the seasons. There is significant variation between wet and dry seasons of Zn, Pb, and Mo (23–174 ng m^{-3}, 35–89 ng m^{-3}, 2.8–13 ng m^{-3}, respectively), while there is a low significant difference in both seasons in the average concentrations of Ti, Cr, Sr, Ni, and Rb (1.1–4.2 ng m^{-3}, 2.3–2.6 ng m^{-3}, 2.2–2.5 ng m^{-3}, 1.7–1.8 ng m^{-3}, and 0.3–0.4 ng m^{-3}, respectively). All these metals in this fraction were mainly a result of combustion processes from the manufacturing industries in the study area, as reported by other studies in similar regions.[19,23,31]

3.5.2 Determination of trace metal sources. The sources of the trace metals in this study were assessed by using the correlation coefficient and principal component analysis (PCA).

3.5.2.1 Correlation analysis

3.5.2.1.1 Coarse particles. The correlation analysis result of the PM_{10} elements is presented in Table S3. All the major elements in PM_{10}, such as K, Ca, and Fe, had a strong positive correlation with one another (r = 0.88–0.96) and with all the trace metals, with their regression coefficient 'r' ranging from 0.53 (K–Rb) to 0.97 (Fe–Ti). This suggests that they have a common origin, which could be mostly attributed to crustal sources. Similarly, there is a very strong positive correlation among all the trace metals with strong regression coefficients from 0.57 (Sr–Ti) to 0.96 (Pb–Mo). This implies that these metals likely had similar origins, which could be geogenic, mixed with anthropogenic.

3.5.2.1.2 Fine fraction. Meanwhile, the metals in $PM_{2.5}$ in Table S3 revealed that K could have a common source with Cu, Mn, Fe, and Zn (r = 0.58–0.82), Fe a similar origin with Cu, Zn, and Pb (0.73–0.75). Only significant correlation exists between Mn and Zn–Fe–Cu–Rb–Pb (r = 0.57–0.92), Mn–Cu (0.76), and Mn–Pb (0.85), while also Zn–Cu (0.75), Zn–Rb (0.64), Zn–Pb (0.79), and Pb–Rb (0.63) had strong positive correlations among the trace metals. These signify that they have a common origin, and they are mostly attributed to anthropogenic origin from combustion processes in MRF plants.

3.5.2.2 PCA analysis. The specific sources of the metals were further identified through PCA, which was carried out on the data set of the metals for both PM_{10} and $PM_{2.5}$ across the seasons (Table 5). The PCA of metals revealed 3 principal components for PM_{10} and 5 for $PM_{2.5}$ that explained 95.35% and 86.04% of the total variability in the size fractions, respectively.

3.5.2.2.1 Coarse fraction (PM_{10}). PC1 described 46.21% of the common variance, and it is characterized by high loading of the typical crustal metals (K, Ca, Fe, Ti, and Mn) and anthropogenic elements (Cr and Zn). Thus, PC1 represents a combined influence of crustal and anthropogenic sources on PM_{10} elemental composition in the study area. The association of Ca, Fe, K, Mn, and Ti with this factor suggests that these elements reflect the local soil composition, which is subsequently resuspended into the atmosphere. The report of Ezeh *et al.*[31] in a similar environment confirmed that the aforementioned crustal elements were preponderant in their PC1 for PM_{10} particle fraction. The source of these elements was also attributed to crustal sources, such as entrained soil dust from poorly maintained road networks and unpaved walkways. The reflection of Cr and Zn in this PC suggests their contribution to industrial combustion. Similarly, Ezeh *et al.*,;[31] Owoade *et al.*,[19] further opined that these elements were inputs from emissions emanating from industrial activities such as smelting work. Also, the presence of Fe and Zn was reported by Olatunji *et al.*,[20] in a similar environment. Their reports revealed the presence of Fe and Zn-rich particles in the coarse mode particulate matter using scanning electron microscopy coupled with energy dispersive X-ray (SEM-EDX) technique. It was established that these particles were also the product of emissions from the MRF plants.

PC2 explained 37.31% of the total variance and was heavily loaded with Ni, Cu, Mo, and Pb. They were mainly emitted from the MRF as described by Owoade *et al.*,.[19] This was attributed to the melting of alloying materials and expended paints from the scrap metals that will become volatile during the smelting process.[27] PC3 describes11.83% of the variance and it is composed of only Sr. This factor was also sourced from crustal origin.

3.5.2.2.2 Fine fractions. The PCA result of fine particulate fraction ($PM_{2.5}$) is presented in Table 5. The PC1 is anthropogenic with 39.20% of the variance and is composed of K, Cu, Ni, Fe, Zn, Mn, and Pb. This is mainly attributed to anthropogenic activities from industrial combustion. PC2 is a crustal factor, accounting for 15.73% of the total variance. It is characterized by high levels of Ca and Sr, which are thought to primarily originate from crustal sources. In contrast, the PC3 is an

Table 5 Principal component analysis of PM_{10} and $PM_{2.5}$in the study area

	PM_{10}			$PM_{2.5}$				
	PC1	PC2	PC3	PC1	PC2	PC3	PC4	PC5
K	0.70	0.37	0.18	0.67	0.56	0.04	0.08	0.24
Ca	0.79	0.39	0.14	0.32	0.56	0.49	−0.07	−0.32
Ti	0.91	0.22	0.21	0.08	0.06	0.94	0.17	0.13
Cr	0.82	0.48	0.16	−0.06	0.09	0.09	−0.02	0.96
Mn	0.87	0.41	0.27	0.97	−0.02	0.06	0.11	−0.05
Fe	0.93	0.28	0.24	0.90	0.04	0.29	−0.08	0.00
Ni	0.36	0.71	0.27	0.38	0.44	−0.10	0.15	0.25
Cu	0.35	0.60	0.34	0.83	0.45	−0.04	−0.14	−0.13
Zn	0.79	0.49	0.31	0.91	0.10	−0.09	0.33	−0.05
Sr	0.35	0.35	0.86	−0.17	0.87	0.10	0.12	0.08
Mo	0.23	0.94	0.21	0.17	0.15	0.15	0.94	−0.01
Pb	0.31	0.87	0.31	0.83	−0.28	0.22	0.34	−0.05
Eigen value	5.55	4.48	1.42	4.70	1.89	1.33	1.22	1.19
% Variance	46.21	37.31	11.83	39.20	15.73	11.07	10.15	9.90
Cumulative %	46.21	83.52	95.35	39.20	54.92	65.99	76.14	86.04

anthropogenic factor that explained 11.07% of the total variance and is predominantly associated with Mo, which is attributed to industrial emissions. PC4 and PC5 exhibited nearly identical variances of 10% each. PC4 is also a crustal factor significantly loaded with Ti, which reflects the composition of the local soil. PC5 with its high levels of Cr is attributed to an anthropogenic factor from industrial processes.

3.6 Enrichment factor

Additionally, the crustal enrichment factor (EF) was utilized to assess the contributions of crustal dust to the elemental concentrations observed in the study area. Titanium was selected as the reference element for this analysis. The composition of the upper continental crust, as outlined by Rudnick and Gao,[60] was used to determine the enrichment factors and the crustal contributions to the elemental concentrations. An EF value greater than 2 but less than 10 indicates moderate enrichment, suggesting that the material may derive from other crustal sources with a composition differing from that of the selected reference element. Elements exhibiting an EF greater than 10 are classified as enriched, while those with an EF below 0.70 indicate depletion relative to the reference composition. Enrichment factors ranging from 0.70 to 2 are regarded as comparable and fall within the error margin of the reference source, suggesting that elements with such factors may have originated from that source. Fig. 3a and b show the average enrichment factors for both PM_{10} and $PM_{2.5}$size fractions and wet and dry seasons for the measured metals in the study area. Based on the classification above, two major groups of metals were identified in all the size fractions and seasons, those that were within 2–10 EF values such as Fe, Ca, K, Sr, and Mn are in the first group, while the second group consists of Cr, Ni, Cu, Se, Zn, Pb, and Mo, in which their EF values were greater than 10.

In the PM_{10} fraction the average EF values of Fe, K, Ca, Sr, and Mn were 1.8, 2.8, 3.8, 3.7, and 4.7, respectively, for the wet season, while in the dry season, their corresponding average were 2.4, 1.0, 1.3, 1.8, and 6.6, respectively (Fig. 3a). Therefore, the EF values of these aforementioned elements are relatively low and classified within low to minimal enrichment. This further confirms the assertion that they were contributed from crustal origin (fugitive soil dust) by the calculated PCA. However, their slight value above 2 in some instances also justifies that there could be a slight contribution from anthropogenic activities such as smelting, work biomass burning, and cement production that are common in the study area.

These assertions were supported by the previous work of Owoade *et al.*,[19] who identified these sets of metals as crustal elements in similar environments and found their slight contribution from smelting and biomass burning using positive matrix factorization (PMF). The average EF values of Cr, Ni, Cu, Zn, Pb, and Mo in the wet season were 70, 95, 262, 3808, 26 257, 31 923, respectively, and 22, 31, 119, 6104, 11 198, and 9869, respectively, in the dry season. Consequently, these elements were very strongly enriched to extremely enriched in PM_{10} in both wet and dry seasons. This is a further confirmation that they are pollutants in the environment and were sourced from anthropogenic activities such as industrial combustion from MFRs, as revealed by PCA.

A similar trend was also observed in $PM_{2.5}$ with the average EF values of the aforementioned crustal elements (Fe, K, Ca, Sr, and Mn) ranging from 1.2 (Fe) to 10.7 (Sr) in the wet season and 1.7 (Fe) to 6.5 (Sr) in the dry season (Fig. 3b). Similarly, these elements are largely sourced from entrained soil dust from poorly maintained road network and unpaved walkway.[31] Also, there could be slight contributions of these elements from anthropogenic activities, especially Sr, for the reason mentioned earlier. Furthermore, the extremely strong EF values of Cr, Ni, Cu, Zn, Pb, and Mo during the wet (93–12964) and dry (63–6052) seasons indicated that they are pollutants and sourced from the anthropogenic origin, mainly from smelting work in the environment.

3.7 Health risk assessments

The statistical summary of non-carcinogenic hazard quotient ingestion (HQ_{ing}), inhalation (HQ_{inh}), dermal (HQ_{dermal}), and

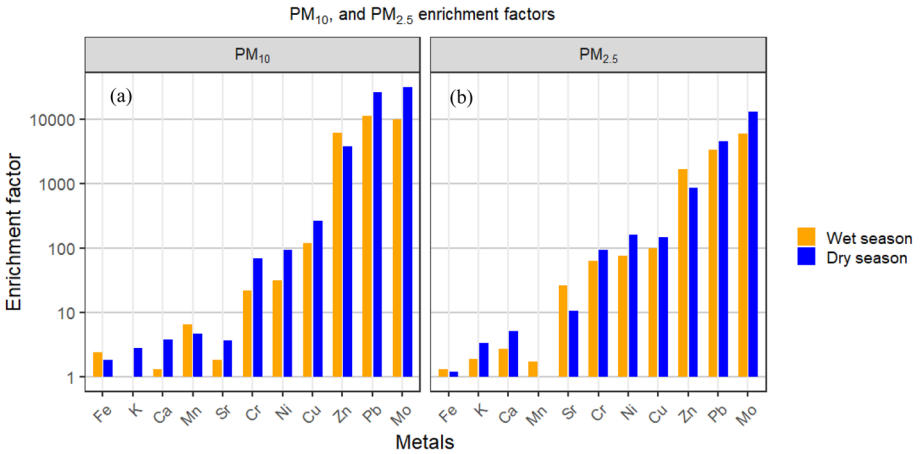

Fig. 3 Enrichment factor of metals in PM_{10} (a) and $PM_{2.5}$ (b) in both wet and dry seasons.

hazard index (HI) estimated on the selected elements such as Cr, Mn, Ni, Cu, Zn, Sr, and Pb in particulate matter in wet and dry seasons for children and adults are presented in Fig. 4 and Tables S4, S5, respectively.

3.7.1 Non-carcinogenic risk

3.7.1.1 Coarse fraction. Based on the average values, the HQs decrease in the following order: $HQ_{ing} > HQ_{dermal} > HQ_{inh}$ in both seasons. Similarly, the HQs of the metals generally decrease in the following order: Pb > Cr > Ni > Cu > Zn > Mn for PM_{10} across the seasons. Furthermore, the highest average HQ_{ing}, HQ_{inh}, and H_{dermal} values were observed for Pb in wet (1.18×10^{-1}, 4.35×10^{-4}, 2.94×10^{-4}, respectively) and dry (3.47×10^{-1}, 1.12×10^{-3}, and 7.53×10^{-4}, respectively) seasons in children (Fig. 4). These HQ values of Pb are in many folds higher than HQs (HQ_{ing}, HQ_{inh}, and HQ_{dermal}) values of Cr, Ni, Cu, and Mn for children (Fig. 4). Likewise, Pb has the highest average HQs values for all the metals in both wet (1.86×10^{21}, 6.57×10^{-5}, 6.59×10^{-5}) and dry (5.46×10^{-2}, 1.68×10^{-4}, and 1.69×10^{-4}) seasons in adults (Fig. 4). Consequently, Pb emerged as the primary factor influencing non-carcinogenic risk across various age demographics. This finding can be attributed to the high concentrations of Pb detected at this location, along with its significant toxicity and corresponding reference dose (RfD) values. Overall, the HQ values for all metals during both the wet and dry seasons were below the permissible threshold of 1 for non-carcinogenic risk, indicating that there is no considerable non-carcinogenic risk to human health. However, the maximum single HQ_{ing} value for Pb (0.82) observed in the dry season for children, which is very close to 1, is worrisome (Table S4). Therefore, progressive exposure to PTEs, especially Pb in the study area, might enhance the non-carcinogenic and carcinogenic risk. Also, when considering the results for the non-carcinogenic risk for both children and adults, it was observed that children had a higher potential risk.

Consequently, the average HI values of the $PM_{10}$for children in the wet (1.20×10^{-1}) and dry (3.56×10^{-1}) seasons and for adults in the respective (1.88×10^{-2} and 5.66×10^{-2}) seasons were less than 1, which indicated that they may pose no significant non-carcinogenic risk (Fig. 4). However, the HI value of 0.83 (Table S4) for children cannot be neglected because continuous emission of PTEs, especially Pb, may pose a significant non-carcinogenic risk in the near future.

3.7.1.2 Fine fraction. A similar trend, such as the order of abundance of $HQ_{ing} > HQ_{dermal} > HQ_{inh}$ and Pb > Cr > Ni > Cu > Zn > Mn for $PM_{2.5}$ across the seasons, was observed in this fraction, except for their lower values compared to PM_{10}. Like PM_{10}, the average HQs values of Pb were also the highest compared to other metals in both the wet (6.51×10^{-3}, 2.37×10^{-5}, 1.60×10^{-5}) and dry (1.70×10^{-2}, 600×10^{-5}, and 4.05×10^{-5}) season for Children (Fig. 4). The respective average HQs (HQ_{ing}, HQ_{inh}, and HQ_{derm}) values for adults were 1.02×10^{-3}, 3.58×10^{-6}, 3.59×10^{-6} in wet season and 2.67×10^{-3}, 9.05×10^{-6}, 9.08×10^{-3} in the dry season (Fig. 4). Also, the HQ values of all the metals in both wet and dry seasons for the children and adults were lower than the maximum allowable limit for non-carcinogenic risk of 1, which poses no significant non-carcinogenic risk to humans. Similarly, the average HI values of the $PM_{2.5}$ for children in the wet (7×10^{-3}) and dry (2.01×10^{-2}) seasons and for adults in the respective (1.10×10^{-3} and 3.16×10^{-3}) seasons were less than 1, which indicated that they may pose no significant non-carcinogenic risk (Fig. 4 and Table S5).

3.7.2 Carcinogenic risk.

The carcinogenic risks (CR) values of Cr, Ni, and Pb for both size fractions (PM_{10} and $PM_{2.5}$) in both seasons (wet and dry seasons) for children are presented in Fig. 4 and Tables S4, S5. The highest average CR values of these elements were observed for Pb in the dry season (1.5×10^{-5}) for PM_{10}, while in $PM_{2.5}$ the highest average CR value of Pb was also found in the dry season (7.3×10^{-7}). It has been established that CR and total carcinogenic risk (TCR) value in the range of 1×10^{-6} – $\times 10^{-4}$ implies an acceptable total risk; risk values < 1×10^{-6} indicate no significant health effects, while values that exceed > 1×10^{-4} indicate unacceptable carcinogenic health risks for humans (Table S4).[61–63] Therefore, all the CR values of the 3 metals were within the acceptable carcinogenic risk. Similarly, the highest average TCR values for children were 2.4×10^{-5} (PM_{10}) and 4.4×10^{-6} ($PM_{2.5}$) observed in the dry

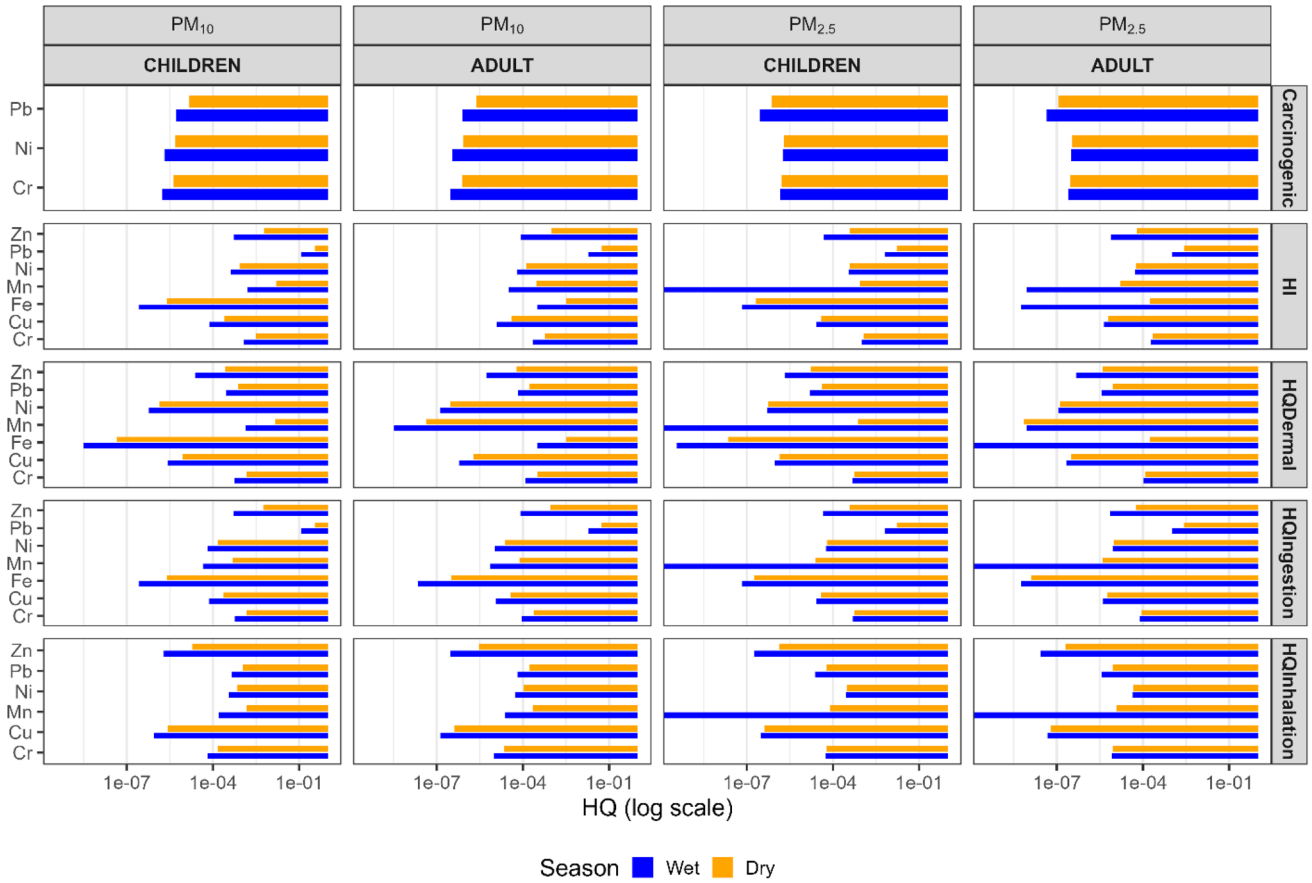

Fig. 4 Average HQ value of non-carcinogenic risk in the three pathways (ingestion, inhalation and dermal), HI, and carcinogenic risk in children and adult.

season. Also, these values were within acceptable limits and posed no significant carcinogenic risk (Fig. 4).

Similar trends of CR values were observed for Cr, Ni, and Pb in adults for both size functions and season, but these values were lower than their corresponding values in children (Fig. 4 and Table S4). Therefore, the range and the average CR values of Cr, Ni, and Pb pose no significant carcinogenic risk to humans in the vicinity of the MRFs (Fig. 4). Likewise, the TCR values were calculated for the adults showed that they were less than the maximum acceptable limit for carcinogenic risk.

4 Conclusions

This study presented the chemical composition of PM_{10} and $PM_{2.5}$ in the wet and dry seasons of metal recycling factories (MRFs) in Nigeria. It also provides the first assessment of human health risks associated with PM_{10} and $PM_{2.5}$ exposure in the MRF environments in Nigeria. Seasonal trends, source contributions, contamination level, and health implications of PM were investigated by evaluating the PM_{10} and $PM_{2.5}$, water-soluble inorganic ions (Cl^-, NO_3^-, and SO_4^{2-}, Na^+, Ca^{2+}, K^+, Mg^{2+}, NH_4^+, $C_2O_4^{2-}$), sugar (Mannosan and Levoglucosan), and metals (Ca, Cr, Cu, Fe, K, Mn, Mo, Ni, Pb Rb, Sr, Ti, and Zn) concentrations. The results show that average $PM_{2.5}$(27 μg m^{-3}) and PM_{10} (109 μg m^{-3}) concentrations exceed World Health Organization (WHO) Air Quality Guidelines especially during the dry season, indicating severe air quality concerns. The elevated levels of Cl^-, NO_3^-, and SO_4^{2-}, Na^+, Ca^{2+}, K^+ were mainly attributed to anthropogenic emissions from the MRFs and biomass burning in the study area. The presence of Levoglucosan also suggests the contribution of regional biomass burning. This study also identifies MRFs as a major contributor to potentially toxic element (PTE) emissions, with elevated levels of elements such as Zn, Cr, and Pb, posing localized risks. The enrichment factors (EFs) of these metals, ranging from 70 to 31 000, further confirm significant to extreme enrichment, indicating a strong anthropogenic influence from the MFRs. In contrast, metals like Ca, K, Na, and Sr exhibited low EFs, suggesting a predominantly crustal origin. The results of the estimated human health risk of PTEs like Cr, Mn, Ni, Cu, Zn, and Pb show no non-carcinogenic risk for most of the metals to children and adults. While most metals pose no significant health risk, lead (Pb) is a notable exception, with hazard quotient and index values close to permissible limits, especially for children. This highlights the need for urgent attention to mitigate Pb pollution and its potential long-term effects on the environment and public health. The study's findings will inform policymakers in enhancing environmental regulations and inspection procedures to ensure cleaner and safer air for the nation.

Author contributions

Tesleem Olalekan Kolawole: writing – original draft, validation, methodology, investigation, formal analysis, conceptualization. Khanneh Wadinga Fomba: writing – original draft, validation, methodology, formal analysis, conceptualization. Hartmut Herrmann: writing – review and editing, validation, supervision, conceptualization. Godwin C. Ezeh: Writing – review and editing, methodology, investigation, conceptualization. Akinade S. Olatunji: writing – review and editing, methodology, investigation, conceptualization. Khaleel A. Ghazal: writing – review and editing, methodology, investigation. Falk Mothes: writing – review and editing, methodology, conceptualization.

Conflicts of interest

The authors declare that they have no known competing financial interests.

Data availability

Data will be made available on request.

The supplementary information (SI) consists of five tables. Tables S1, S4, and S5 provides information on the reference dose values of heavy metals, and the non-carcinogenic human health risk assessment for children and adults, respectively. Tables S2 and S3 reports the correlation coefficient between water-soluble ions and between the reported trace metals in PM_{10} and $PM_{2.5}$, respectively. See DOI: **https://doi.org/10.1039/d5ea00045a**.

Acknowledgements

These trace metal results are part of a project that has received funding from the European Union's Horizon 2020 research and innovation programme under grant agreement No. 730997.

References

1 X. Cheng, Y. Huang, S. Zhang, S. Ni and Z. Long, Characteristics, Sources, and Health Risk Assessment of Trace Elements in PM_{10} at an Urban Site in Chengdu, Southwest China, *Aerosol Air Qual. Res.*, 2018, **18**, 357–370.

2 D. Pavlović, M. Pavlović, V. Perović, Z. Mataruga, D. Čakmak, M. Mitrović and P. Pavlović, Chemical Fractionation, Environmental, and Human Health Risk Assessment of Potentially Toxic Elements in Soil of Industrialised Urban Areas in Serbia, *Int. J. Environ. Res. Public Health*, 2021, **18**, 9412, DOI: **10.3390/ijerph18179412**.

3 T. O. Kolawole, O. M. Ajibade, J. O. Olajide-Kayode and K. W. Fomba, Level, distribution, ecological, and human health risk assessment of heavy metals in soils and stream sediments around a used-automobile spare part market in Nigeria, *Environ. Geochem. Health*, 2023, **45**, 1573–1598, DOI: **10.1007/s10653-022-01283-z**.

4 K. W. Fomba, O. L. Faboya, N. Deabji, A. Makhmudov, J. Hofer, E. J dos Santos Souza, K. Müller, D. Althausen, S. Sharipov, S. Abdullaev and H. Herrmann, The seasonal variation of Asian dust, anthropogenic PM, and their sources in Dushanbe, Tajikistan, *Atmos. Environ.*, 2024, **333**, 120667.

5 A. G. Allen, E. Nemitz, J. P. Shi, R. M. Harrison and J. C. Greenwood, Size distributions of trace metals in atmospheric aerosols in the United Kingdom, *Atmos. Environ.*, 2001, **35**, 4581–4591.

6 I. B. Obioh, G. C. Ezeh, O. E. Abiye, A. Alpha, E. O. Ojo and A. K. Ganiyu, Atmospheric particulate matter in Nigerian megacities, *Environ. Toxicol. Chem.*, 2013, **95**, 379–385.

7 United Nation Environment Programme/World Health Organization (UNEP/WHO), *GEMS/AIR Methodology Reviews 1, Suspended Particulate Matter in Ambient Air*, WHO/EOS/94.3, UNEP/GEMS/94.A.4, UNEP, Nairobi, Kenya, 1994.

8 T. D. Tran, P. M. Nguyen, D. T. Nghiem, T. H. Le, M. B. Tu, L. Y. Alleman, V. M. Nguyen, D. T. Pham, N. M. Ha, M. N. Dang, C. V. Le and N. V. Nguyen, Assessment of Air Quality in School Environments in Hanoi, Vietnam: A Focus on Mass-Size Distribution and Elemental Composition of Indoor-Outdoor Ultrafine/Fine/Coarse Particles, *Atmosphere*, 2020, **11**, 519.

9 World Health Organisation (WHO), Health Aspects of Air Pollution with Particulate Matter, Ozone and Nitrogen Dioxide, *Report on a WHO Working Group Meeting Bonn, 13-15 January, 2003*, WHO Regional Office for Europe, Copenhagen, 2003.

10 Health Effects Institute (HEI), *State of Global Air*, 2019, DOI: **10.1080/02772248.2013.790970**, **https://www.stateofglobalair.org/**.

11 W. Phairuang, M. Inerb, M. Hata and M. Furuuchi, Characteristics of trace elements bound to ambient nanoparticles (PM0.1) and a health risk assessment in southern Thailand, *J. Hazard. Mater.*, 2022, **425**, 127986.

12 J. A. Adeniran, R. O. Yusuf and A. A. Olajire, Exposure to coarse and fine particulate matter at and around major intra-urban traffic intersections of Ilorin metropolis, Nigeria, *Atmos. Environ.*, 2017, **166**, 383–392doi, DOI: **10.1016/j.atmosenv.2017.07.041**.

13 J. Bachwenkizi, C. Liu, X. Meng, L. Zhang, W. Wang, A. van Donkelaar, R. V. Martin, M. S. Hammer, R. Chen and H. Kan, Fine particulate matter constituents and infant mortality in Africa: A multicountry study, *Environ. Int.*, 2021, **156**, 106739.

14 G. Rushingabigwi, P. Nsengiyumva, L. Sibomana, C. Twizere and W. Kalisa, Analysis of the atmospheric dust in Africa: the breathable dust's fine particulate matter $PM_{2.5}$ in correlation with carbon monoxide, *Atmos. Environ.*, 2020, **224**, 117319.

15 J. A. Adesina, S. J. Piketh, M. Qhekwana, R. Burger, B. Language and G. Mkhatshwa, Contrasting indoor and ambient particulate matter concentrations and thermal comfort in coal and non-coal burning households at South Africa Highveld, *Sci. Total Environ.*, 2019, **699**, 134403, DOI: **10.1016/j.scitotenv.2019.134403**.

16 S. E. West, P. Büker, M. Ashmore, G. Njoroge, N. Welden, C. Muhoza, P. Osano, J. Makau, P. Njoroge and W. Apondo, Particulate matter pollution in an informal

settlement in Nairobi: Using citizen science to make the invisible visible, *Appl. Geogr.*, 2020, **114**, 102133.
17 O. L. Faboya, K. W. Fomba and H. Herrmann, Organic and Elemental Carbon in PM2.5 from an Urban Residential Area of Lagos, Nigeria, *Adv. Sci. Technol. Innov.*, 2024, 13–17.
18 T. O. Kolawole, J. O. Olajide-Kayode, L. A. Azeez, K. W. Wadinga, M. T. Jimoh, M. O. Raheem and I. A. Oyediran, Health risk assessment of potentially toxic elements in dust and soils of used lead-acid battery shops, *Int. J. Environ. Sci. Technol.*, 2025, **22**, 13961–13980.
19 K. O. Owoade, P. K. Hopke, P. S. Olise, L. T. Ogundele, O. G. Olaniyi, B. H. Fawole and O. O. Jegede, Chemical compositions and source identification of particulate matter ($PM_{2.5}$ and $PM_{2.5-10}$) from a scrap iron and steel smelting industry along the Ife–Ibadan highway, Nigeria, *Atmos. Pollut. Res.*, 2015, **6**, 107–119.
20 A. S. Olatunji, T. O. Kolawole, M. Oloruntola and G. Günter, Evaluation of pollution of soils and particulate matter around metal recycling factories in southwestern Nigeria, *J. Health. Pollut.*, 2018, **8**, 20–30, DOI: **10.5696/2156-9614-8.17.20**.
21 M. Schindler, M. Santosh, G. Dotto, L. F. O. Silva and M. F. Hochella Jr, A review on Pb-bearing nanoparticles, particulate matter and colloids released from mining and smelting activities, *Gondwana Res.*, 2021, **110**, 330–346.
22 R. E. Showman and S. B. Harmon, US. Pat. No. 8, B2, 426493, 2013.
23 K. O. Owoade, F. S. Olise, I. B. Obioh, H. B. Olaniyi, L. Ferrero and E. Bolzacchini, EDXRF elemental assay of airborne particulates: A case study of an iron and steel smelting industry, Lagos, Nigeria, *Sci. Res. Essays*, 2009, **4**, 1342–1347.
24 R. A. Street, W. Goessler, S. Naidoo, B. Shezi, N. Cele, J. Rieger, K. Ettinger, T. Reddy and A. Mathee, Exposure to lead and other toxic metals from informal foundries producing cookware from scrap metal, *Environ. Res.*, 2020, **191**, 109860.
25 K. Zhang, F. Chai, Z. Zheng, Q. Yang, X. Zhong, K. W. Fomba and G. Zhou, Size distribution and source of heavy metals in particulate matter on the lead and zinc smelting affected area, *J. Environ. Sci.*, 2018, **71**, 188–196, DOI: **10.1016/j.jes.2018.04.018**.
26 W. Phairuang, T. Chetiyanukornkul, P. Suriyawong, S. Ho, P. Paluang, M. Furuuchi, M. Amin and M. Hata, Daytime-nighttime variations in the concentration of PM0.1 carbonaceous particles during a biomass fire episode in Chiang Mai, Thailand, *Particuology*, 2024, **87**, 316–324.
27 A. F. I. Apanpa-Qasim, A. A. Adeyi, S. N. Mudliar, K. Raghunathan and P. Thawale, Examination of Lead and Cadmium in Water-based Paints Marketed in Nigeria, *J. Public Health Policy*, 2016, **6**, 43–49.
28 H. Wang, L. Cai, H. Wang, G. Hu and L. Chen, A comprehensive exploration of risk assessment and source quantification of potentially toxic elements in road dust: A case study from a large Cu smelter in central China, *Catena*, 2021, **196**, 104930.
29 M. Mowla, E. Rahman, N. Islam and N. Aich, Assessment of heavy metal contamination and health risk from indoor dust and air of informal E-waste recycling shops in Dhaka, Bangladesh, *J. Hazard. Mater. Adv.*, 2021, **4**, 100025.
30 C. C. Ibebuchi and I. Abu, Rainfall variability patterns in Nigeria during the rainy season, *Sci. Rep.*, 2023, **13**, 7888, DOI: **10.1038/s41598-023-34970-7**.
31 G. C. Ezeh, I. B. Obioh, O. I. Asubiojo and O. E. Abiye, PIXE characterization of PM_{10} and $PM_{2.5}$ particulates sizes collected in Ikoyi Lagos, Nigeria, *Toxicol. Environ. Chem.*, 2015, **94**, 884–894, DOI: **10.1080/02772248.2012.674133**.
32 P. K. Hopke, Y. Xie, T. Raunema, S. Biegalski, S. Landsberger and D. Cohen, Characterization of the Gent stacked filter unit PM10 sampler, *Aerosol Sci. Technol.*, 1997, **27**, 726–735.
33 K. W. Fomba, N. Deabji, S. E. Barcha, I. Ouchen, E. Elbaramoussi, R. C. El Moursli, M. Harnafi, S. El Hajjaji, A. Mellouki and H. Herrmann, Application of TXRF in monitoring trace metals in particulate matter and cloud water, *Atmos. Meas. Tech.*, 2020, **13**, 4773–4790, DOI: **10.5194/amt-2019-428**.
34 S. Zeppenfeld, M. van Pinxteren, A. Engel and H. Herrmann, A protocol for quantifying mono- and polysaccharides in seawater and related saline matrices by electro-dialysis (ED) – Combined with HPAEC-PAD, *Ocean Sci.*, 2020, **16**, 817–830.
35 K. W. Fomba, K. Müller, D. van Pinxteren, L. Poulain, M. van Pinxteren and H. Herrmann, Long-term chemical characterization of tropical and marine aerosols at the Cape Verde Atmospheric Observatory (CVAO) from 2007 to 2011, *Atmos. Chem. Phys.*, 2014, **14**, 8883–8904, **https://acp.copernicus.org/articles/14/8883/2014/doi:10.5194/acp-14-8883-2014**.
36 D. van Pinxteren, V. Engelhardt, F. Mothes, L. Poulain, K. W. Fomba, G. Spindler, A. Cuesta-Mosquera, T. Tuch, T. T. Müller, A. Wiedensohler, G. Löschau, S. Bastian and H. Herrmann, Residential Wood Combustion in Germany: A Twin-Site Study of Local Village Contributions to Particulate Pollutants and Their Potential Health Effects, *ACS Environ. Au*, 2023, **4**, 12–30, DOI: **10.1021/acsenvironau.3c00035**.
37 USDOE, *The Risk Assessment Information System (RAIS). Cass Avenue Argonne*, IL, U.S. Department of Energy's Oak Ridge Operations Office (ORO), 2011.
38 U.S. Environmental Protection Agency (USEPA), *Risk Assessment Guidance for Superfund, Vol I., Human Health Evaluation Manual (Part A) Office of Emergency and Remedial Response*, Washington, 1989.
39 T. O. Kolawole and A. S. Olatunji, Assessment of concentration of the potentially toxic elements and associated human health risk from particulate matter exposure along road intersections in Ibadan, southwestern Nigeria, *Discov. Environ.*, **1**, 3, DOI: **10.1007/s44274-023-00005-1**.
40 J. O. Olajide-Kayode, T. O. Kolawole, O. O. Oyaniran, S. O. Mustapha and A. S. Olatunji, Potentially Harmful Element toxicity in Geophagic clays consumed in parts of southeastern Nigeria, *J. Trace Elem. Min.*, 2023, **4**, 100050, DOI: **10.1016/j.jtemin.2023.100050**.

41 K. W. Fomba, K. Müller, J. Hofer, A. N. Makhmudov, D. Althausen, B. I. Nazarov, S. F. Abdullaev and H. Herrmann, Variations of the aerosol chemical composition during Asian dust storm at Dushanbe, Tajikistan, *E3S Web Conf.*, 2019, **99**, 03007.

42 H. Chu, H. Yu and Y. Kuo, Identifying spatial mixture distributions of PM2.5 and PM10 in Taiwan during and after a dust storm, *Atmos. Environ.*, 2012, **54**, 728–737.

43 C. Y. Hsu, H. Chiang, S. Lin, M. Chena, T. Lin and Y. Chen, Elemental characterization and source apportionment of PM10 and PM2.5 in the western coastal area of central Taiwan, *Sci. Total Environ.*, 2016, **541**, 1139–1150.

44 K. Zhang, F. Chai, Z. Zheng, Q. Yang, X. Zhong, K. W. Fomba and G. Zhou, Size distribution and source of heavy metals in particulate matter on the lead and zinc smelting affected area, *J. Environ. Sci.*, 2018, **71**, 188–196, DOI: **10.1016/j.jes.2018.04.018**.

45 J. Lim, J. Lee, J. Moon, Y. Chung and K. Kim, Airborne PM10 and metals from multifarious sources in an industrial complex area, *Atmos. Res.*, 2010, **96**, 53–64.

46 M. A. Zoran, R. S. Savastru, D. M. Savastru and M. N. Tautan, Assessing the relationship between surface levels of PM2.5 and PM10 particulate matter impact on COVID-19 in Milan, Italy, *Sci. Total Environ.*, 2020, **738**, 139825.

47 Q. Guo, K. Chen and G. Xu, Characteristics and Sources of Water-Soluble Inorganic Ions in PM2.5 in Urban Nanjing, China, *Atmosphere*, 2023, **14**, 135, DOI: **10.3390/atmos14010135**.

48 E. Chianese, G. Tirimberio, A. Dinoi, D. Cesari, D. Contini, P. Bonasoni, A. Marinoni, V. Andreoli, V. Mannarino and S. Moretti, Ionic and Elemental Composition of Particulate Matter during the Winter Season: A Comparative Study among Rural, Urban and Remote Sites in Southern Italy, *Atmosphere*, 2022, **13**, 356.

49 P. Bhuyan, M. Ahmed, P. K. Hopke and R. R. Hoque, Understanding the Chemistry and Sources of Precipitation Ions in the mid-Brahmaputra Valley of Northeastern India, *Aerosol Air Qual. Res.*, 2020, **20**, 2690–2704.

50 B. R. T Simoneit, J. J. Schauer, C. G. Nolte, D. R. Oros, V. O. Elias, M. P. Fraser, W. F. Rogge and G. R. Cass, Levoglucosan, a tracer for cellulose in biomass burning and atmospheric particles, *Atmos. Environ.*, 1999, **33**(2), 173–182.

51 G. Schkolnik, A. H. Falkovich, Y. Rudich, W. Maenhaut and P. Artaxo, New analytical method for the determination of levoglucosan, polyhydroxy compounds and 2-methylerythritol and its application to smoke and rainwater samples, *Environ. Sci. Technol.*, 2005, 2744–2752.

52 M. Viana, C. Reche, F. Amato, A. Alastuey, X. Querol, T. Moreno, F. Lucarelli, S. Nava, G. Cazolai, M. Chiari and M. Rico, Evidence of biomass burning aerosols in the Barcelona urban environment during winter time, *Atmos. Environ.*, 2008, **72**, 81–88.

53 H. Stevens, L. A. Barmuta, Z. Chase, K. M. Saunders, A. Zawadzkic, A. R. Bowie, M. M. G. Perron, E. Sanz Rodriguez, B. Paull, D. P. Child, M. A. C. Hotchkis and B. C. Proemse, Comparing levoglucosan and mannosan ratios in sediments and corresponding aerosols from recent Australian fires, *Sci. Total Environ.*, 2024, **945**, 174068.

54 S. L. Mkoma, K. Kawamura and P. Q. Fu, Contributions of biomass/biofuel burning to organic aerosols and particulate matter in Tanzania, East Africa, based on analyses of ionic species, organic and elemental carbon, levoglucosan and Mannosan, *Atmos. Chem. Phys.*, 2013, **13**, 10325–10338.

55 G. C. Ezeh, I. B. Obioh, O. I. Asubiojo, M. Chiari, S. Nava, G. Calzolai, F. Lucarelli and C. Nuviadenu, The complementarity of PIXE and PIGE techniques: A case study of size segregated airborne particulates collected from a Nigeria city, *Appl. Radiat. Isot.*, 2012, **201**(103), 82–92.

56 S. L. Mkoma, W. Maenhaut, X. Chi, W. Wang. and N. Raes, Characterisation of PM10 atmospheric aerosols for the wet season 2005 at two sites in East Africa, *Atmos. Environ.*, 2009, **43**, 631–639.

57 V. E. Toledo, Evaluation of levels, sources and distribution of toxic elements in PM10 in a suburban industrial region, Rio de Janeiro, Brazil, *Environ. Monit. Assess.*, 2008, 49–59.

58 K. W. Fomba, K. Muller, D. van Pinxteren and H. Herrmann, Aerosol size-resolved trace metal composition in remote northern tropical Atlantic marine environment: case study Cape Verde islands, *Atmos. Chem. Phys.*, 2013, **13**, 4801–4814. **https://acp.copernicus.org/articles/13/4801/2013/doi:10.5194/acp-13-4801-2013**.

59 M. F. Soto-Jiméneza and A. R. Flegal, Metal-contaminated indoor and outdoor housedust from a neighborhood Smelter area in Torreón, Mexico, *Procedia Environ. Sci.*, 2011, **4**, 134–137.

60 R. L. Rudnick and S. Gao, Composition of the continental crust. in. *Treatise on geochemistry: The crust*, ed. R. L. Rudnick, 683, Elsevier Ltd, Oxford, 2003.

61 P. C. Agyeman, K. John, N. M. Kebonye, L. Borůvka, R. Vašát, O. Drábek and K. Němeček, Human health risk exposure and ecological risk assessment of potentially toxic element pollution in agricultural soils in the district of FrydekMistek, Czech republic: A sample location approach, *Environ. Sci. Eur.*, 2021, **33**, 1–25.

62 H. Baltas, M. Sirin, E. Gokbayrak and A. E. Ozcelik, A case study on pollution and a human health risk assessment of heavy metals in agricultural soils around Sinop province Turkey, *Chemosphere*, 2020, **241**, 125015.

63 J. C. Agbasi, C. N. Chukwu, N. D. Nweke, H. C. Uwajingba, M. Y. A. Khan and J. C. Egbueri, Water pollution indexing and health risk assessment due to PTE ingestion and dermal absorption for nine human populations in Southeast Nigeria, *Groundw. Sustain. Dev.*, 2023, **21**, 100921.